



PROCESSING OF β -TYPE BIOMEDICAL $Ti_{74}Nb_{26}$ ALLOY BY COMBINATION OF HOT PRESSING AND HIGH TEMPERATURE SINTERING

¹Tarık AYDOĞMUŞ^{ID}, ²Nuaman Jasim Filamarz Al-ZANGANA^{ID}, ³Fevzi KELEN^{ID}

^{1,2}Van Yüzüncü Yıl University, Engineering Faculty, Mechanical Engineering Department, Van, TURKEY

²Sulaimani Polytechnic University, Technical College of Engineering, Sulaimani, IRAQ

³Van Yüzüncü Yıl University, Van Vocational School, Department of Motor Vehicles and Transport Technologies, Van, TURKEY

¹aydogmus@yyu.edu.tr, ²nuaman.zangana@spu.edu.iq, ³fkelen@yyu.edu.tr

(Geliş/Received: 05.07.2019; Kabul/Accepted in Revised Form: 06.11.2019)

ABSTRACT: Titanium (Ti)-Niobium (Nb) alloys are generally produced by casting methods. Since the melting temperatures of pure Ti and Nb are quite high, their fabrication by casting techniques is costly. On the other hand, it is possible to produce these alloys economically at much lower temperatures (less than melting temperature of Ti), completely in solid state using powder metallurgy. In the present study, $Ti_{74}Nb_{26}$ alloys were produced using pure Ti and pure Nb powders by combination of hot pressing and high temperature sintering for the first time. The influences of processing temperature and time on density, microstructure, and mechanical behavior were investigated. Density measurements showed that hot pressing at 800 °C provided full density. XRD and SEM investigations revealed that amount of β phase formed increased with increasing sintering time. In addition to main phase β , little amount of α phase and a very small amount of pure Nb were observed in the microstructure. Mechanical properties were measured by means of uniaxial compression and micro Vickers indentation tests. The results indicated that 4 h of sintering at 1200 °C exhibited the highest value of hardness (336 HV), elastic modulus (44 GPa), yield strength (894 MPa), and compressive strength (1178 MPa).

Key Words: Titanium-Niobium alloys, Powder metallurgy, Hot pressing, Sintering, Microstructure, Mechanical properties.

Sıcak Presleme Ve Yüksek Sıcaklık Sinterleme Kombinasyonu İle B Tipi Biyomedikal $Ti_{74}Nb_{26}$ Alaşımının Üretimi

ÖZ: Ti-Nb alaşımları genellikle döküm yöntemi ile üretilirler. Saf Ti ve Nb'un erime sıcaklıkları oldukça yüksek olduğundan döküm yoluyla Ti-Nb alaşımlarını üretmek maliyetlidir. Toz metalurjisi yöntemi ile bu alaşımları çok daha düşük sıcaklıklarda (Ti erime sıcaklığından daha az) ve tamamen katı halde ekonomik olarak üretmek mümkündür. Bu çalışmada $Ti_{74}Nb_{26}$ alaşımları saf Ti ve saf Nb tozları kullanılarak, sıcak presleme ve yüksek sıcaklık sinterlemesinin ilk kez birlikte uygulanması ile üretilmiştir. Üretim sürecinde uygulanan işlem sıcaklığı ve zamanının yoğunluk, mikroyapı ve mekanik davranış üzerindeki etkileri araştırılmıştır. Yoğunluk ölçümleri, 800 °C'de yapılan sıcak presleme işleminin tam yoğunluğu sağladığını göstermiştir. XRD ve SEM incelemeleri, sinterleme süresinin artmasıyla birlikte β fazı oluşumunun arttığını ortaya koymuştur. Ana faz β 'ya ilaveten, mikroyapıda az miktarda α fazı ve çok az miktarda saf Nb gözlenmiştir. Mekanik özellikler tek eksenli basma ve mikro Vickers sertlik testleri ile belirlenmiştir. Mekanik test sonuçları, 1200 °C'de 4 saatlik sinterlemenin en yüksek sertlik (336 HV), elastik modül (44 GPa), akma mukavemeti (894 MPa) ve basma mukavemeti (1178 MPa) değerlerini sağladığını göstermiştir.

Anahtar Kelimeler: Titanyum-Niobyum alaşımları, Toz metalurjisi, Sıcak presleme, Sinterleme, Mikroyapı, Mekanik özellikler

1. INTRODUCTION

Stainless steels, cobalt based alloys and Ti alloys are the most widely used metallic biomaterials. Among them Ti alloys show the highest biocompatibility, specific strength and corrosion resistance. The use of Ti alloys is not limited only to the biomaterials industry they are also used in aerospace applications since they have numerous favorable mechanical properties, such as good fatigue strength, high wear resistance, excellent fracture toughness and high strength to weight ratio compared to other materials or alloys (Elias *et al.*, 2006; Niinomi *et al.*, 2012; Zhuravleva *et al.*, 2013; Cremasco *et al.*, 2013; Sharma *et al.*, 2016).

Inadequate wear resistance, high oxidation at elevated temperatures, low hardness and low yield strength of pure Ti reduce the lifetime of parts and limit fields of its application (Shymanski *et al.*, 2015). Varying physical, chemical and mechanical properties for Ti alloys can be achieved by alloying Ti with several metallic elements, such as aluminum (Al), vanadium (V), iron (Fe), tin (Sn), molybdenum (Mo), chromium (Cr), zirconium (Zr), tantalum (Ta) and Nb. In order to solve the toxicity problems of some alloying elements, such as nickel (Ni), Al and V new Ti alloys were suggested (Niinomi *et al.*, 2012). These new metastable β -Ti alloys, such as Ti-Nb, Ti-Ta and Ti-Zr show considerable promise due to their superior properties including lower elastic moduli, higher strength, good ductility and compositions absent of potentially cytotoxic elements. Among them Ti-Nb based alloys display the lowest elastic moduli and better shape memory effect (Kim *et al.*, 2006; Niinomi *et al.*, 2012; Kent *et al.*, 2013). Pure Nb is a completely biocompatible material and doesn't cause any tissue reaction. Young's modulus of Ti alloys can be reduced by adding Nb acting as a β -phase stabilizing element in Ti alloys (Wang and Zheng, 2009; Niinomi *et al.*, 2012; Zhao *et al.*, 2013; Zhao *et al.*, 2015). Nb also increase the resistance of Ti to oxidation and contributes to decrease of oxygen solubility and further oxygen diffusion into the alloy (Han *et al.*, 2015). These properties make Ti-Nb alloys faithful and possible candidate biomedical materials for replacing frequently used commercial Ti6Al4V and TiNi alloys (Kim *et al.*, 2006; Wang and Zheng 2009; McMahon *et al.*, 2012; Kent *et al.*, 2013; Andrade *et al.*, 2015; Bönisch *et al.*, 2015; Prokoshkin *et al.*, 2016).

Ti-Nb alloys are generally produced by casting techniques (Hon *et al.*, 2003; Ozaki *et al.*, 2004; Kim *et al.*, 2006; Chai *et al.*, 2008; Chai *et al.*, 2009; Ma *et al.*, 2010; Cremasco *et al.*, 2013; Han *et al.*, 2015; Bönisch *et al.*, 2015; Prokoshkin *et al.*, 2016). Porosity, rough microstructure, and composition segregation are the main defects normally present by casting and greatly worsen the mechanical properties. Also, melting points of Ti and Nb, 1668 and 2477 °C, respectively, are extremely high that special furnaces (vacuum arc melting, VAM and vacuum induction melting, VIM), too much energy and expensive equipments such as vacuum are needed to produce Ti-Nb alloys via casting methods. Expensive machining operations and high cost of raw materials are other cost-increasing factors. Significant cost reductions can be achieved by using powder metallurgy techniques to get near net shapes while reducing processing temperature and machining time and material waste. Ti-Nb based alloys can be manufactured by powder metallurgical processing techniques using elemental powders, since they require relatively low temperatures (less than melting point of Ti) for sintering compared to higher casting temperatures needed for VAM or VIM.

The objective of the present study is to fabricate and characterize bulk Ti₇₄Nb₂₆ alloy which is a promising candidate material for metallic implant applications. The reason for choosing this composition is that it has the lowest elastic modulus value, ~60 GPa, (Ozaki *et al.*, 2004) among Ti-Nb binary alloys very important to prevent or minimize stress shielding effect occurring as a result of the mismatch between elastic modulus of the implant material and that of bone (less than 30 GPa, Li *et al.*, 2014) and may results in loosening of the implant. The alloy has been produced combining hot pressing (for full densification) and high temperature sintering (for Nb dissolution in Ti and accordingly to obtain β phase) for the first time since the previous studies such as carried out by Santos *et al.*, 2005 reported that conventional or pressureless powder metallurgy methods could not achieve full density and could not get rid of the porosity completely even for sintering temperatures as high as 1600 °C.

2. MATERIALS and METHODS

In the present study, elemental pure Ti (99.5%) and pure Nb (99.8 %) powders (both of them smaller than 45 μm and supplied by Alfa Aesar, Germany) were used to fabricate Ti-40Nb (wt. %) corresponding to Ti₇₄Nb₂₆ alloy by at. %. Scanning electron microscope (SEM) images given in Figure 11 show the morphological properties of as-received powders. The shapes of Ti and Nb powder particles were irregular since they were produced hydride dehydride conversion technique.

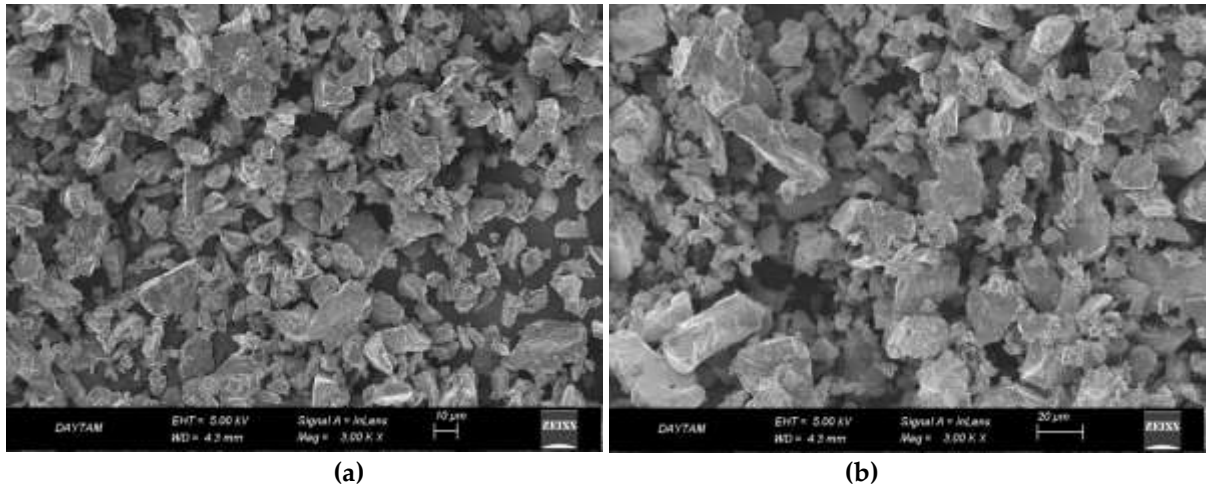


Figure 1. SEM micrographs of pure (a) Ti and (b) Nb powders.

Figure 2 presents the X-Ray Diffraction (XRD) results of starting raw powders. The phases existing in the microstructure of Ti and Nb powders were pure α -Ti with a hexagonal close packed (HCP) crystal structure and pure Nb with a body centered cubic (BCC) structure. None of the powders contained oxide or carbide phases so that they were free from any type of contamination.

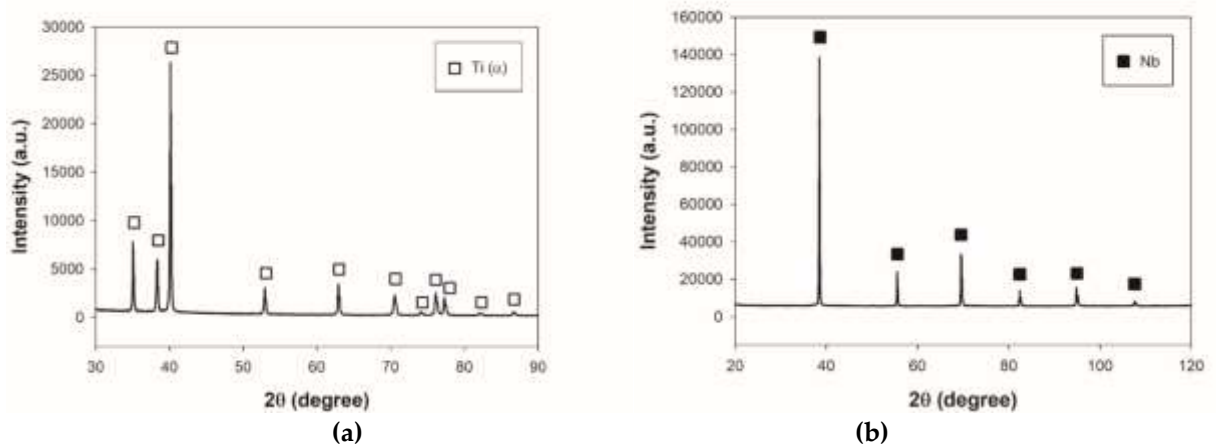


Figure 2. XRD patterns of as-received (a) Ti powders and (b) Nb powders

Composition of the Ti-Nb alloy is selected to be Ti₇₄Nb₂₆ because this composition has the lowest elastic modulus value as stated before. Weights of raw powders were calculated considering the selected composition and final dimensions of the cylindrical samples (15 mm in diameter and 10 mm in height). It was assumed that hot pressed samples would attain full density (zero porosity) in order to get the predetermined height or thickness of 10 mm. Powders were weighted using an electronic balance and mixed manually with the help of a binder, ethylene, for 15 minutes to obtain a homogeneous mixture. Afterwards, the mixture was charged into a hollow cylindrical graphite die with inner diameter of 15 mm.

The graphite die tool filled with Ti and Nb powder mixture was put into the pressing chamber. Then the door of hot pressing chamber was closed and the chamber was vacuumed. Following vacuuming the chamber was filled with pure argon gas. This procedure was repeated 3 times and all the residual air was swept away from the chamber. Specimens were heated to the hot pressing temperatures predetermined, pressed and sintered at those temperatures simultaneously for 1 h of constant time. The pressure applied during heating, pressing and cooling steps kept constant as 50 MPa. An MSE_M_HP_1300 model hot press was employed to produce samples and hot pressing operation was carried out at 600 °C, 650 °C and 800 °C. All the hot pressing experiments were done under flowing argon gas atmosphere to prevent oxidation of samples. Finally, hot pressed samples were left to cooling inside the chamber and taken from the chamber when the temperature decreased to 150 °C. The graphite deposited as a thin layer on the hot pressed sample surfaces were removed applying grinding for which a wheel rotating type machine (Struers Labo Pol 5) and 240 and 320 grit SiC papers were used. After grinding, samples were cleaned in an ultrasonic cleaner for 10 minutes to remove possible residues and left drying. Next, samples put in an alumina (Al_2O_3) crucible were further sintered at 1200 °C in a vertical tube furnace (Protherm PTF 14/50/450) for 1, 2, 3 and 4 h under flowing argon gas to obtain desired β phase providing Nb dissolution in Ti. Sintering temperature (1200 °C) was kept constant for all the specimens. After sintering, the samples were furnace cooled and removed from the furnace at 200 °C. Heating, sintering and cooling curves are given in Figure 3. Temperature-time curve of hot pressing has also been added into that figure for comparison. Initial linear region in the curves represents heating step where the heating rates were kept constant as 10 and 8 °C/min for hot pressing and sintering, respectively. Horizontal second region corresponds to hot pressing or sintering time and finally the third region shows the cooling step where the slopes of the curves at different points are variable, not constant. This means that cooling rate is not constant during cooling; it is maximum just after sintering completed (at the beginning of the cooling stage) and decreases with time.

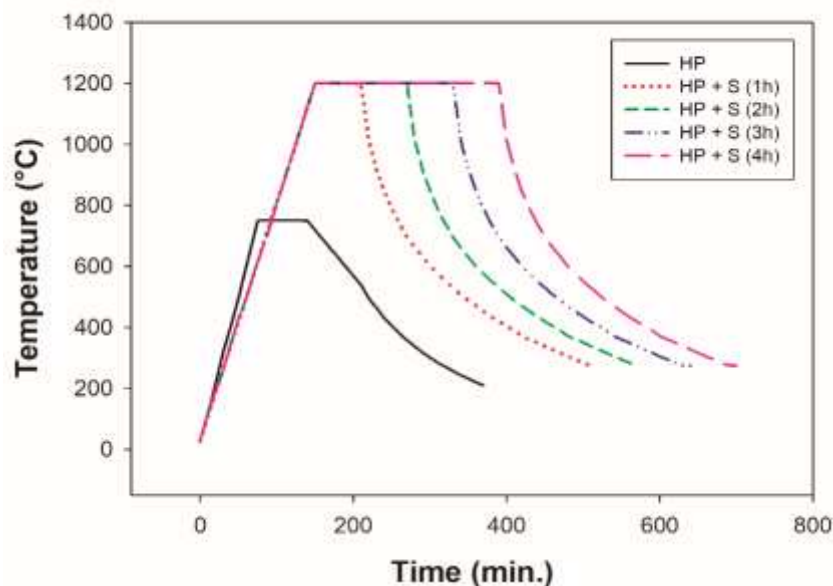


Figure 3. Temperature-time curves of hot pressing (HP) for 1h and following sintering (HP+S) processes for different times.

Density and the porosity of the samples in hot pressed and sintered conditions were measured using Archimedes' principle employing an electronic precision balance (X Precisa 321) equipped with a density determination kit by using the water replacement (suspension) method.

The samples for microstructural and mechanical characterization were cut in the dimensions of 5x5x10 mm using electrical discharge machine systems (EDM), Charmilles Robofil 290 and 310. Samples in

compression tests were used as they were cut. For XRD studies surface of the samples were grinded with 320 SiC papers to remove contamination residues left after cutting operation. For micro hardness and SEM investigations specimens were subjected to full metallographic preparation steps in which grinding (240-1200 grinding papers), polishing (diamond suspension, 3 μm) and finally etching was applied, respectively. Kroll's reagent (3 ml HF + 6 ml HNO₃ + 100 ml H₂O) was used to etch the samples for about 15 seconds.

XRD analysis were carried out using a PANalytical Empyrean model X-ray diffractometer with CuK α radiation ($\lambda=1.540598 \text{ \AA}$) at 45 kV, 40 mA within a range of diffraction angles 2θ from 20° to 90° at a scan speed of 2 degree/min. Microscopic investigation was performed by a Zeiss Sigma 300 SEM equipped with an energy dispersive spectroscopy (EDS) detector. Both secondary electron (SE) and backscattered electron (BSE) modes were applied to identify the different phases in the microstructure. Compositional analysis was done employing EDS point analysis technique.

Vickers hardness was measured on the polished specimens using a digital micro hardness tester (HVD-1000AP) with a load of 100 g force (981 mN) and 20 second dwell time. Uniaxial compression tests at ambient temperature ($25 \pm 5 \text{ }^\circ\text{C}$) were conducted using a universal Raagen tension-compression testing device. Elastic modules were determined by applying least squares curve fitting to the linear portion of the stress-strain diagram while yield strengths of the sintered samples were determined using the 0.2%-offset method. Compression strengths were the maximum stresses achieved and as a measure of ductility fracture strains were used. Both surfaces of the compression test specimens were mechanically ground to render them parallel. Graphite was used to reduce friction between the samples and the compression plates and also to prevent or minimize barreling during uniaxial compression testing.

3. RESULTS and DISCUSSION

Theoretical density of Ti₇₄Nb₂₆ alloy is calculated as 5.578 g/cm³. Measured density and calculated porosity of the samples in hot pressed and sintered conditions are shown in Table 1. The density of the sample hot pressed at 600 °C was only 4.52 g/cm³ and its porosity was close to 17%. 50 °C increment in hot pressing temperature decreased the porosity to 12.5% so that hot pressing temperature was increased to 800 °C providing almost full density. Hot pressing at 800 °C resulted in a porosity of only 0.85%. This little amount of porosity would be eliminated during following high temperature sintering. Consequently, hot pressing temperature was optimized to be 800 °C and all the samples were pressed at that temperature prior to sintering. Actually, this was the idea behind combining hot pressing with high temperature sintering. Previous studies (Santos *et al.*, 2005) present in the literature showed that, conventional cold pressing and sintering could not eliminate all the porosity. On the other hand, only hot pressing is not sufficient for complete dissolution of Nb in Ti and accordingly getting β phase desired due to its limited temperature. As expected sintering carried out for different times eliminated the porosity remained from hot pressing and full density was achieved for all the sintering durations of 1 to 4 h.

Table 1. Density and porosity of the samples produced in different conditions

Specimen	Density (g/cm ³)	Porosity (%)
600 °C 1h (HP)	4.52	16.89
650 °C 1h (HP)	4.88	12.53
800 °C 1h (HP)	5.53	0.85
1200 °C 1h (HP+S)	5.58	0
1200 °C 2h (HP+S)	5.59	0
1200 °C 3h (HP+S)	5.59	0
1200 °C 4h (HP+S)	5.60	0

XRD patterns of the sintered samples revealed that β phase formed as a result of Nb dissolution in Ti as it can be seen from Figure 4 4. In addition to main phase β (BCC) little amount of α phase (HCP) were

also detected in the microstructure. Longer sintering times increased the intensity of β peaks while those of α phases decreased. Even 4 h of sintering at 1200 °C was not enough to eliminate all the α phase and to get single β phase. Nevertheless, amount of α phase was very low which can be seen comparing main peak intensities of two phases.

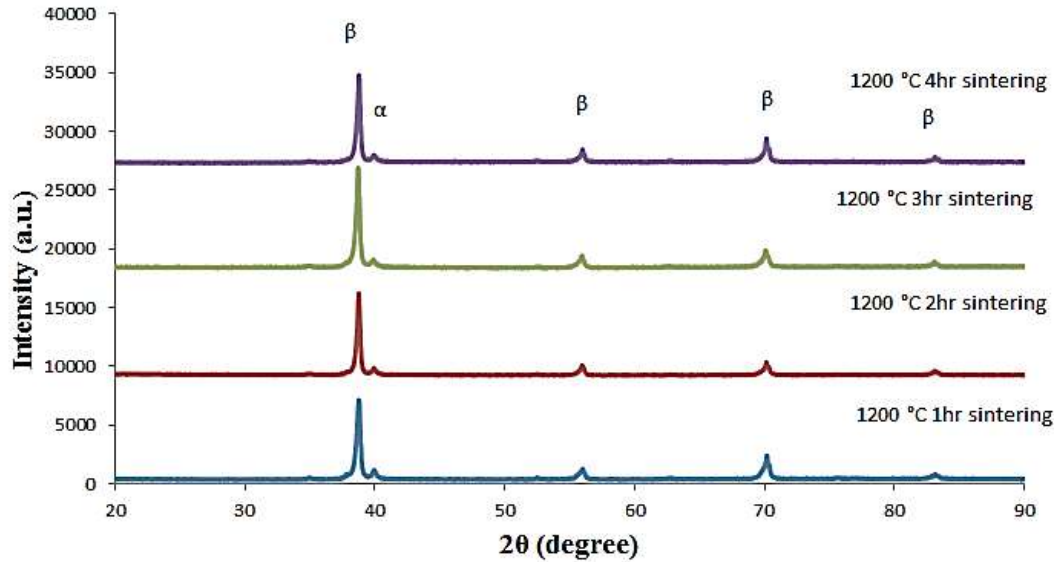


Figure 4. XRD patterns of specimens hot pressed at 800 °C for 1h and then sintered at 1200 °C for different times

The morphological characteristics of the sintered samples at 1200 °C for different times after hot pressing at 800 °C for 1h were examined with the SEM and the microstructures are presented in Figure 5. SEM micrographs revealed that with increasing sintering time from 1h to 4h amount of α phase decreased and the amount of β phase increased. The results were in good agreement with those obtained from XRD. EDS point analysis revealed that Nb contents of the α (Figure 5e) and β phase (Figure 5f) were 4.3 ± 0.5 (at. %) and 26.1 ± 3 (at. %), respectively.

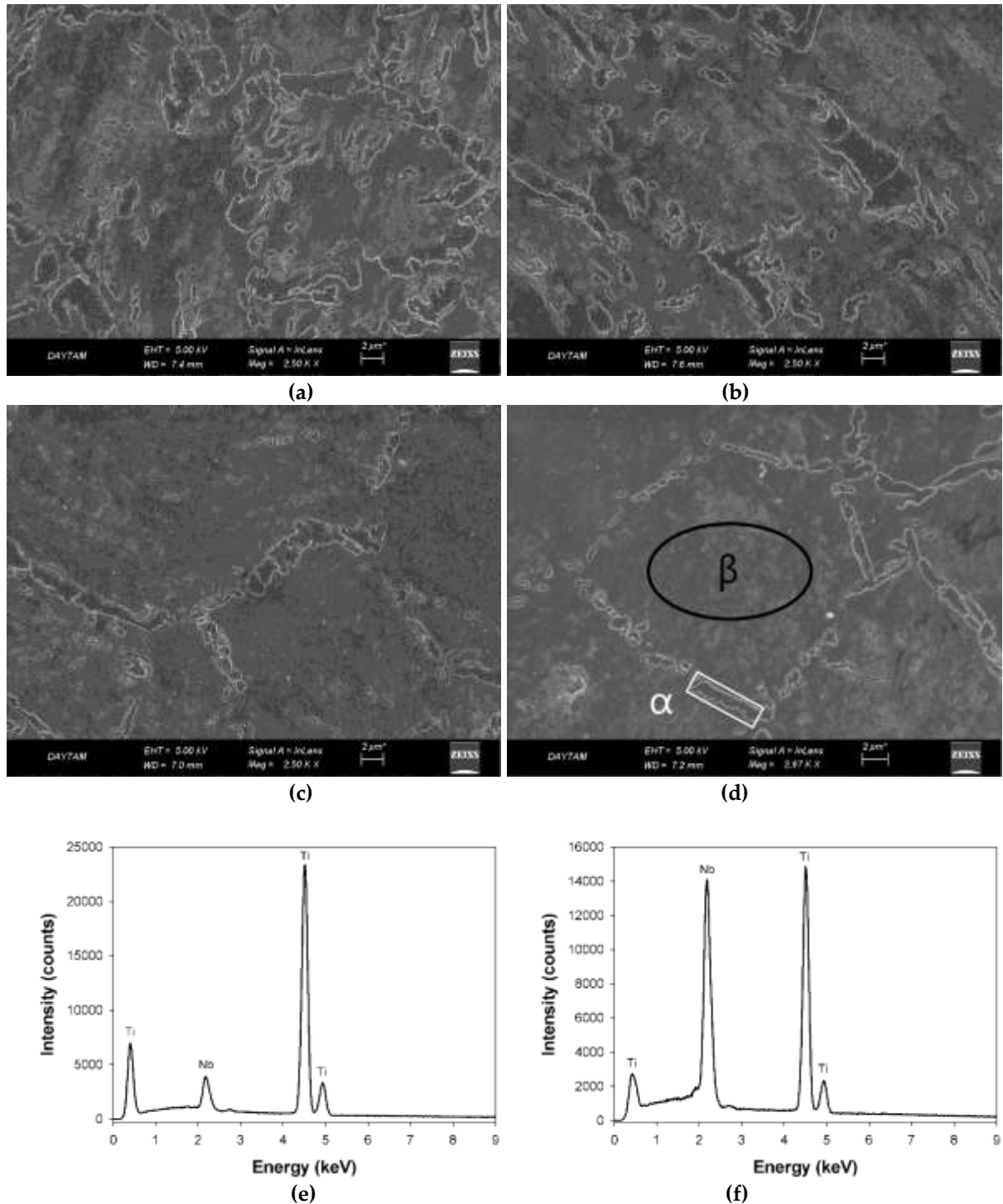


Figure 5. SEM images of Ti₇₄Nb₂₆ alloy sintered for (a) 1h, (b) 2h, (c) 3h and (d) 4h at 1200 °C and EDS point analysis results of (e) α phase and (f) β phase both shown in (d)

BSE mode was used in order to ensure whether undissolved pure Nb existed or not in the microstructure of the samples since it was quite difficult to differentiate in SE mode. BSE micrographs of bulk Ti₇₄Nb₂₆ alloys are given in Figure 6. The micrographs are similar and the microstructure consists of the same phases. The amount of α phase is very small as detected by XRD and SE mode in SEM, β is the main phase and a little undissolved pure Nb in white color was also observed. EDS point analysis given in Figure 6e proves that all the white regions in BSE images correspond to pure Nb. Although amount of

pure Nb decreased with increasing sintering time its complete elimination was not possible by sintering at 1200 °C even for the longest sintering time of 4h used in the present study.

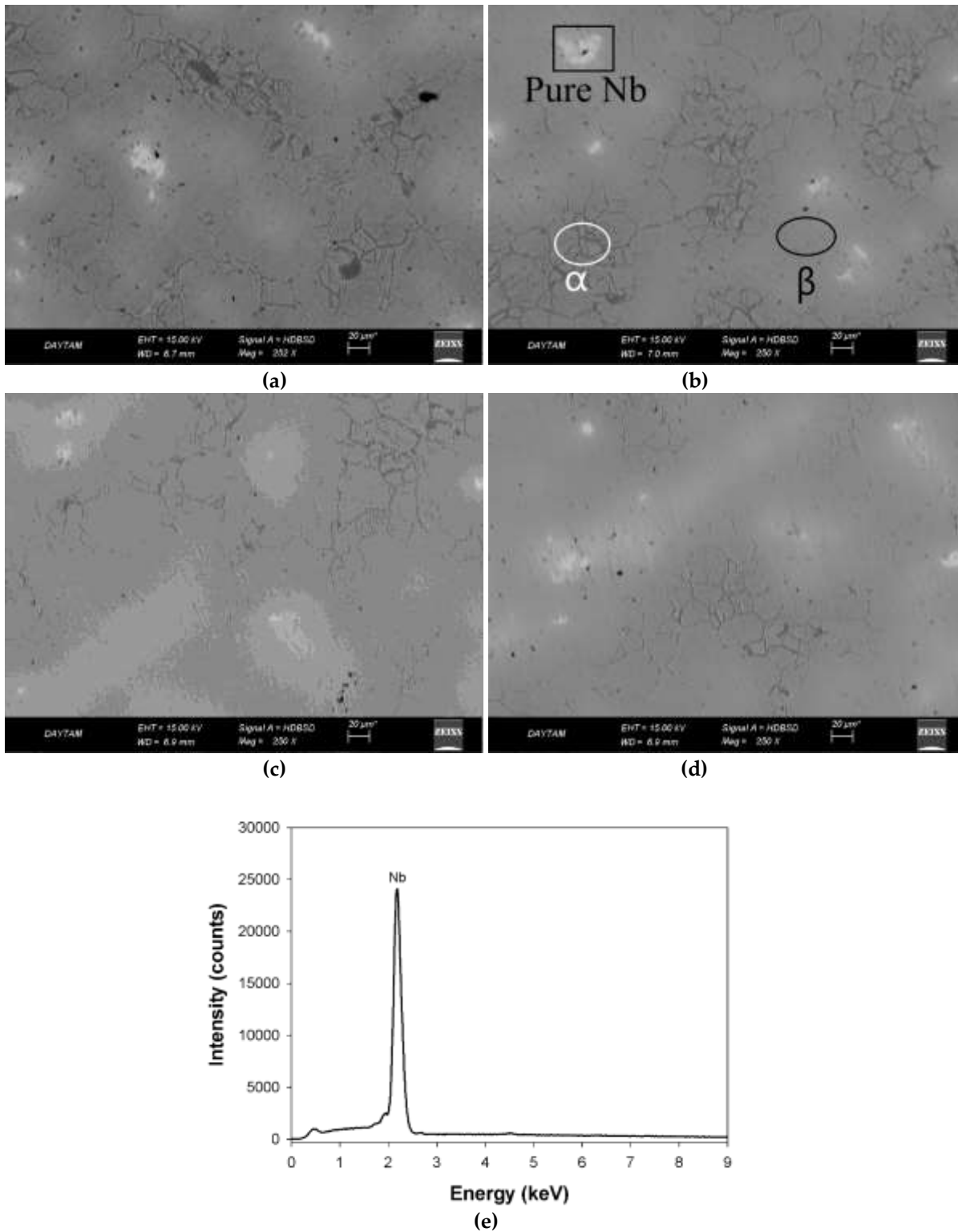


Figure 6. BSE micrographs of bulk Ti₇₄Nb₂₆ sintered at 1200 °C for (a) 1h, (b) 2h, (c) 3h and (d) 4h. (e) EDS point analysis result of white region shown in (b).

The micro hardness values presented a clear relation with sintering duration. Longer sintering times resulted in higher hardness as observed in Table 2. As expected, 4h of sintering at 1200 °C exhibited the

highest hardness value of 332 HV. The lowest hardness measured was 309 HV of 1h sintered sample at the same temperature. Increase in sintering time increased the amount of β phase which is harder than α phase (Lee *et al.*, 2002) and consequently, hardness value also increased.

Table 2. Vickers micro hardness tests results

Sintering time (h)	1	2	3	4
Mean Hardness (HV)	308.8 ± 21.1	315 ± 20.8	330.8 ± 29.2	332 ± 3.1

Figure 7 presents the stress-strain curves of sintered samples at 1200 °C for different times. Mechanical properties obtained from these curves are summarized in Table 3. Young's modulus of the samples sintered for 1, 2, 3 and 4h were 40, 41, 41.4 and 44 GPa, respectively as shown in Table 3. The lowest yield strength was measured to be 789 MPa for 1h sintered sample and increased with increasing sintering time up to 894 MPa for the sample sintered for 4h. Compressive strength values were also increased from 1020 (1h) to a maximum of 1178 MPa (4h). Fracture strains as a measure of ductility were very similar for all the sintering times and changing in the range of 18-21%. The value of elastic modulus (44 GPa), yield strength (894 MPa) and compression strength (1178 MPa) were the highest mechanical properties all obtained for 4 hours of sintering.

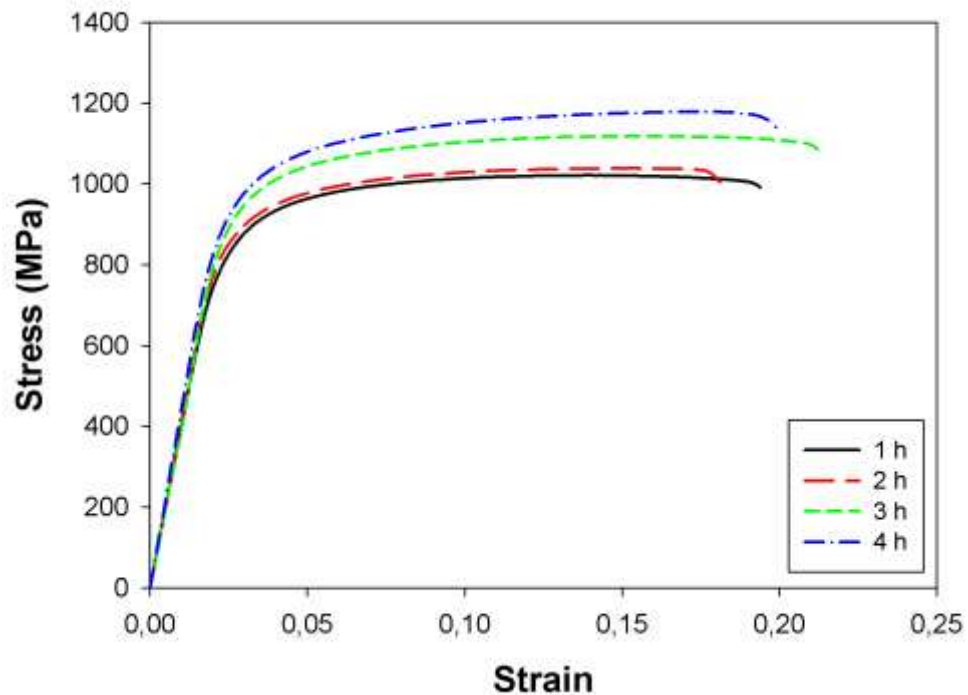


Figure 7. Stress-strain curves of sintered samples at 1200 °C for different times

Table 3. Mechanical properties of Ti₇₄Nb₂₆ alloys sintered at 1200 °C for variable times

Sintering time (h)	Elastic modulus (GPa)	Yield strength (MPa)	Compression strength (MPa)	Fracture strain (%)
1	40.1	789	1020	19.4
2	41	803	1038	18.1
3	41.4	856	1118	21.3
4	44	894	1178	19.9

The relations between mechanical properties and sintering time are plotted in Figure 8. Elastic modulus increases as the sintering time gets longer since the extended sintering times provides better bonding between the initial powders. However, in the present study increase of Young's modulus was only 4 GPa with the increment of sintering time from 1h to 4h. This is due to low elastic modulus of β phase. α has a higher elastic modulus and longer sintering times decreased the α phase amount. As a result, the increase in elasticity modulus was limited just too a few GPas. Yield and compressive strengths enhanced especially after 2h of sintering. This can be understood comparing the slope of the linear curves between 1 and 2h, and after 2h up to 4h. As it can be seen from Figure 8b the slope of the both curves increase after 2h. In addition to higher amount of β phase (Figure 5 and Figure 6), longer sintering times promote additional particle-to-particle bonding. Therefore, yield and compression strength of the samples increase with increasing sintering time.

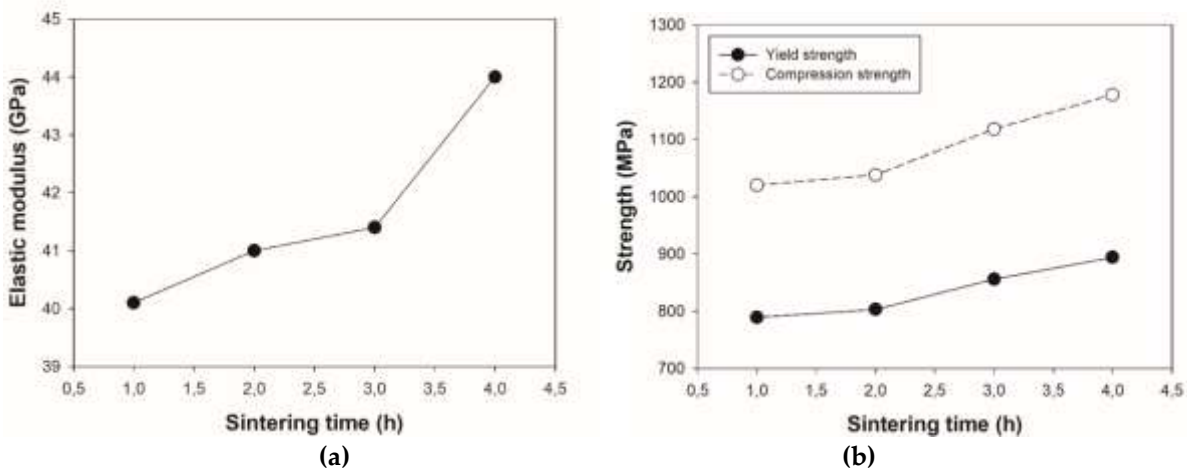


Figure 8. (a) Elastic modulus, (b) yield and compressive strength as a function of sintering time

In Table 4 mechanical properties of the samples produced in the present study has been compared to the results published already. The sample hot pressed at 800 °C for 1h and sintered at 1200 °C for 4h exhibited the lowest Young's modulus (44 GPa) and highest yield strength (894 MPa). It is clear from the table that, similar compositions (highlighted with bold style in the table) produced with casting methods resulted in elastic modulus values of 45-95 GPa. Yield strength values (250-722 MPa) on the other hand were quite low compared to the results of the present study. Hardness values were also in the range of (188-323 HV) comparable to our result of 332 HV. As a result, it can be concluded that hot pressing following high temperature sintering is a quite efficient method to produce bulk Ti-Nb alloys with superior mechanical properties. The mechanical properties of Ti-Nb alloys produced by other powder metallurgy techniques, although in different compositions, are also shown in the table to give an idea.

Table 4. Comparison of mechanical properties with the ones existing in the literature

Composition	Elastic Modulus (GPa)	Yield strength (MPa)	Hardness (HV)	Fabrication method and condition		Reference
Ti-35Nb (wt. %)	94.9 ± 5.7	722 ± 21	323 ± 15	VAM, HT @ 1000 °C, 24h	Furnace Cooled	Cremasco <i>et al.</i> , 2010
	75.2 ± 15.7	343 ± 1	188 ± 4		Water Quenched	
Ti-10Nb (wt. %)	85.2±9.0	552±19	MIM, 1500 °C, 4h		Zhao <i>et al.</i> , 2013
Ti-16Nb (wt. %)	78.4±5.6	589±20			
Ti-22Nb (wt. %)	70.9±7.2	649±31			
Ti-10Nb (wt. %)	90.1±6.1	612±3.6	MIM, 1500 °C, 4h + HIP, 915 °C, 2h		Zhao <i>et al.</i> , 2013
Ti-16Nb (wt. %)	82.2±5.0	661±14			
Ti-22Nb (wt. %)	75.6±7.6	687±34			
Ti-24Nb (at. %)	50	250	CCIM + HT @ 950 °C, 20h + CW 95% reduction in thickness + ST @ 900 °C, 1h		Elmay <i>et al.</i> , 2014
Ti-26Nb (at. %)	45	300			
Ti-26Nb (at. %)	44	894	332	HP @ 800 °C, 1h + S @ 1200 °C, 4h		Present study

VAM: Vacuum Induction Melting, HT: Homogenization Treatment, MIM: Metal Injection Molding, HIP: Hot Isostatic Pressing
CCIM: Cold Crucible Induction Melting or Cold Crucible Levitation Melting, CW: Cold work, ST: Solutionizing Treatment

4. CONCLUSIONS

In this study, binary Ti₇₄Nb₂₆ alloys were produced combining, for the first time, hot pressing with high temperature sintering. General conclusions obtained from the study are as follows:

- Density measurements (Archimedes' technique) showed that optimum hot pressing temperature of Ti-Nb alloys for 1h is 800 °C. Almost full density (over 99%) was achieved at 800 °C.
- The microstructures of Ti₇₄Nb₂₆ alloys sintered at 1200 °C for different times consist of small amount of α and very little undissolved pure Nb in addition to the main phase β and amount of β increases with increasing sintering time according to XRD and SEM investigations.
- Even 4 h of sintering at 1200 °C was not sufficient to obtain single β phase. Therefore, sintering temperature should be higher than 1200 °C to get only β phase free from α and pure Nb.
- Mechanical properties enhanced by increasing sintering time. 4h of sintering exhibited the highest mechanical properties including elastic modulus (44 GPa), yield strength (894 MPa), compression strength (1178 MPa) and microhardness (332 HV). Ductility (18-21%) on the other hand was almost the same for all the sintering temperatures.
- Samples produced combining hot pressing and high temperature sintering were found to be suitable in terms of mechanical properties for bone replacement applications although they have higher elastic modulus (40-44 GPa) compared to that of bone ($E_{bone} < 30$ GPa).

REFERENCES

- Andrade, D.P., Vasconcellos, L.M.R., Carvalho, I.C.S., Forte, L.F.B.P., Santos, E.L.S., Prado, R.F., Santos, D.R., Cairo, C.A.A., Carvalho, Y.R., 2015, "Titanium-35Niobium Alloy as a Potential Material for Biomedical Implants: In vitro Study", *Materials Science and Engineering C*, Vol. 56, pp. 538-544.
- Bönisch M., Calin, M., Humbeek, J.V., Skrotzki, W., Eckert, J., 2015, "Factors Influencing the Elastic Moduli, Reversible Strains and Hysteresis Loops in Martensitic Ti-Nb Alloys", *Materials Science and Engineering C*, Vol. 48, pp. 511-520.

- Chai, Y.W., Kim, H.Y., Hosoda, H., Miyazaki, S., 2008, "Interfacial Defects in Ti-Nb Shape Memory Alloys", *Acta Materialia*, Vol. 56, pp. 3088-3097.
- Chai, Y.W., Kim, H.Y., Hosoda, H., Miyazaki, S., 2009, "Self-accommodation in Ti-Nb Shape Memory Alloys", *Acta Materialia*, Vol. 57, pp. 4054-4064.
- Cremasco, A., Ferreira, I., Caram R., 2010, "Effect of Heat Treatments on Mechanical Properties and Fatigue Behavior of Ti-35Nb Alloy Used as Biomaterial", *Materials Science Forum*, Vol. 636-637 pp. 68-75.
- Cremasco, A., Lopes, E.S.N., Cardoso, F.F., Contieri, R.J., Ferreira, I., Caram, R., 2013, "Effects of the Microstructural Characteristics of a Metastable β Ti Alloy on its Corrosion Fatigue Properties", *International Journal of Fatigue*, Vol. 54, pp. 32-37.
- Elias, L.M., Schneider, S.G., Schneider, S., Silva, H.M., Malvisi, F., 2006, "Microstructural and Mechanical Characterization of Biomedical Ti-Nb-Zr (-Ta) Alloys", *Materials Science and Engineering A*, Vol. 432, No. 1-2, pp. 108-112.
- Elmay, W., Patoor, E., Gloriant, T., Prima, F., Laheurte, P., 2014, "Improvement of Superelastic Performance of Ti-Nb Binary Alloys for Biomedical Applications", *Journal of Materials Engineering and Performance*, Vol. 23, No. 7, pp. 2471-2476.
- Han, M.K., Kim, J.Y., Hwang, M.J., Song, H.J., Park Y.J., 2015, "Effect of Nb on the Microstructure, Mechanical Properties, Corrosion Behavior, and Cytotoxicity of Ti-Nb Alloys", *Materials*, Vol. 8, No. 9, pp. 5986-6003.
- Hon, Y.H., Wang, J.Y., Pan, Y.N., 2003, "Composition/Phase Structure and Properties of Titanium-Niobium Alloys", *Materials Transactions*, Vol. 44, No. 11, pp. 2384-2390.
- Kent, D., Wang, G., Dargusch, M., 2013, "Effects of Phase Stability and Processing on the Mechanical Properties of Ti-Nb based β Ti Alloys", *Journal of the Mechanical Behavior of Biomedical Materials*, Vol. 28, pp. 15-25.
- Kim, H.Y., Kim, J.I., Inamura, T., Hosoda, H., Miyazaki, S., 2006, "Effect of Thermo-mechanical Treatment on Mechanical Properties and Shape Memory Behavior of Ti-(26-28) at.% Nb Alloys", *Materials Science and Engineering A*, Vol. 438-440, pp. 839-843.
- Lee, C.M., Ju, C.P., Chern Lin, J.H., 2002, "Structure-property relationship of cast Ti-Nb alloys", *Journal of Oral Rehabilitation*, Vol. 29, No. 4, pp. 314-322.
- Li, Y., Yang, C., Zhao, H., Qu, S., Li, X., Li, Y., 2014, "New Developments of Ti-based Alloys for Biomedical Applications", *Materials*, Vol. 7, No. 3, pp. 1709-1800.
- Ma, J., Karaman, I., Maier H.J., Chumlyakov, Y.I., 2010, "Superelastic Cycling and Room Temperature Recovery of Ti₇₄Nb₂₆ Shape Memory Alloy", *Acta Materialia*, Vol. 58, pp. 2216-2224.
- McMahon, R.E., Ma, J., Verkhoturov, S.V., Munoz-Pinto, D., Karaman, I., Rubitschek, F., Maier, H.J., Hahn, M.S., 2012, "A Comparative Study of the Cytotoxicity and Corrosion Resistance of Nickel-Titanium and Titanium-Niobium Shape Memory Alloys", *Acta Biomaterialia*, Vol. 8, No. 7, pp. 2863-2870.
- Niinomi, M., Nakai, M., Hieda, J., 2012, "Development of New Metallic Alloys for Biomedical Applications", *Acta Biomaterialia*, Vol. 8, No. 11, pp. 3888-3903.
- Ozaki, T., Matsumoto, H., Watanabe, S., Hanada, S., 2004, "Beta Ti Alloys with Low Young's Modulus", *Materials Transactions*, Vol. 45, No. 8, pp. 2776-2779.
- Prokoshkin, S., Brailovski, V., Dubinskiy, S., Zhukova, Y., Sheremetyev, V., Konopatsky, A., Inaekyan, K., 2016, "Manufacturing, Structure Control, and Functional Testing of Ti-Nb-Based SMA for Medical Application", *Shape Memory and Superelasticity*, Vol. 2, No. 2, pp. 130-144.
- Santos, D.R., Henriques, V.A.R., Cairo, C.A.A., Pereira, M.S., 2005, "Production of a Low Young Modulus Titanium Alloy by Powder Metallurgy", *Materials Research*, Vol. 8, No. 4, pp. 439-442.
- Sharma, B., Vajpai, S.K., Ameyama, K., 2016, "Microstructure and Properties of Beta Ti-Nb Alloy Prepared by Powder Metallurgy Route Using Titanium Hydride Powder", *Journal of Alloys and Compounds*, Vol. 656, pp. 978-986.

- Shymanski, V.I., Cherenda, N.N., Uglov, V.V., Astashynski, V.M., Kuzmitski, A.M., 2015, "Structure and Phase Composition of Nb/Ti System Subjected to Compression Plasma Flow Impact", *Surface & Coatings Technology*, Vol. 278, pp. 183-189.
- Wang, Y.B., Zheng, Y.F., 2009, "Corrosion Behaviour and Biocompatibility Evaluation of Low Modulus Ti-16Nb Shape Memory Alloy as Potential Biomaterial", *Materials Letters*, Vol. 63, pp. 1293-1295.
- Zhao, D., Chang, K., Ebel, T., Qian, M., Willumeit, R., Yan, M., Pyczak, F., 2013, "Microstructure and Mechanical Behavior of Metal Injection Molded Ti-Nb Binary Alloys as Biomedical Material", *Journal of the Mechanical Behavior of Biomedical Materials*, Vol. 28, pp. 171-182.
- Zhao, D., Chang, K., Ebel, T., Nie, H., Willumeit, R., Pyczak, F., 2015, "Sintering Behavior and Mechanical Properties of a Metal Injection Molded Ti-Nb Binary Alloy as Biomaterial", *Journal of Alloys and Compounds*, Vol. 640, pp. 393-400.
- Zhuravleva, K., Bönisch, M., Prashanth, K.G., Hempel, U., Helth, A., Gemming, T., Calin, M., Scudino, S., Schultz, L., Eckert, J., Gebert, A., 2013, "Production of Porous β -Type Ti-40Nb Alloy for Biomedical Applications: Comparison of Selective Laser Melting and Hot Pressing", *Materials*, Vol. 6, No. 12, pp. 5700-5712.